AN AIRFOIL FOR GENERAL AVIATION APPLICATIONS

by

Michael S. Selig
Mark D. Maughmer
Pennsylvania State University
Department of Aerospace Engineering
233 Hammond Bldg.
University Park, PA 16802
and
Dan M. Somers
NASA Langley Research Center
Hampton, VA 23665-5225

For presentation to the AIAA/FAA Joint Symposium on General Aviation Systems at the Port O-Call Inn, Ocean City, NJ on April 12, 1990

AN AIRFOIL FOR GENERAL AVIATION APPLICATIONS

Michael S. Selig † and Mark D. Maughmer ‡
The Pennsylvania State Univeristy
Department of Aerospace Engineering
233 Hammond Bldg.
University Park, PA, 16802

Dan M. Somers §
NASA Langley Research Center
Hampton, VA, 23665-5225

ABSTRACT

A new airfoil, the NLF(1)-0115, has been recently designed at the NASA Langley Research Center for use in general-aviation applications. During the development of this airfoil, special emphasis was placed on experiences and observations gleaned from other successful general-aviation airfoils. For example, the flight lift-coefficient range is the same as that of the turbulent-flow NACA 23015 airfoil. Also, although beneficial for reducing drag and having large amounts of lift, the NLF(1)-0115 avoids the use of aft loading which can lead to large stick forces if utilized on portions of the wing having ailerons. Furthermore, not using aft loading eliminates the concern that the high pitching-moment coefficient generated by such airfoils can result in large trim drags if cruise flaps are not employed.

The NASA NLF(1)-0115 has a thickness of 15%. It is designed primarily for general-aviation aircraft with wing loadings of 718 to 958 N/m^2 (15 to 20 lb/ft^2). Low profile drag as a result of laminar flow is obtained over the range from $c_l = 0.1$ and $R = 9 \times 10^6$ (the cruise condition) to $c_l = 0.6$ and $R = 4 \times 10^6$ (the climb condition). While this airfoil can be used with flaps, it is designed to achieve $c_{l,max} = 1.5$ at $R = 2.6 \times 10^6$ without flaps. The zero-lift pitching moment is held at $c_{m_o} = -0.055$. The hinge moment for a .20c aileron is fixed at a value equal to that of the NACA 63_2-215 airfoil, $c_H = -0.00216$. The loss in $c_{l,max}$ due to leading edge roughness, rain, or insects at $R = 2.6 \times 10^6$ is 11% as compared with 14% for the NACA 23015.

INTRODUCTION

With increasing use of modern/composite structures in general-aviation aircraft, it is possible to obtain tolerances and levels of surface smoothness such that the use of laminar flow airfoils can result in significant gains in aircraft performance[1]. In the past, some of the attempts to use such airfoils were not fully successful. For example, the loss of the laminar flow due to surface contamination, etc. sometimes resulted in a significant reduction in the maximum lift coefficient which could produce very dangerous situtations with regard to take-off and landing. Also causing concern was the fact that some earlier laminar-flow airfoils were aft pressure

---

† Graduate Assistant, Student Member AIAA
‡ Assistant Professor, Senior Member AIAA
§ Currently with Airfoils, Inc., 601 Cricklewood Dr., State College, PA, 16801

loaded in order to have long regions of favorable pressure gradients resulting in significant runs of laminar flow. For some applications, the use of such airfoils can result in trim-drag penalties due to large nose-down pitching moments. Likewise, if such airfoils are used over the regions of the wings in which control surfaces are located, large control forces can exist and the control surfaces can have a tendency to "float."

Using the experience obtained with laminar-flow airfoils over the years, a new airfoil has been developed which provides the performance gains possible with laminar flow but without the concerns associated with some of the earlier efforts. The result of this design effort is an airfoil having performance better than those traditionally used for such applications while not giving up any of the desirable characteristics of those older airfoils.

AIRFOIL DESIGN

OBJECTIVES AND CONSTRAINTS

Many of the design requirements for a modern general-aviation airfoil can be derived from other successful general-aviation airfoils. Most notably the turbulent-flow NACA 23015 airfoil[2] has been a popular choice for general-aviation applications for many years. This fact stems not only from the broad lift range and low pitching moment, but also from small loss in $c_{l,max}$ due to surface contamination. The laminar-flow NACA 63_2-215 airfoil[2] has also had wide appeal owing to its low-drag, yet it suffers from a narrow usable lift range as compared with the NACA 23015.

The principle goal of this airfoil-design effort is to maintain the lift range of the NACA 23015 while realizing low-drag characteristics like those of the NACA 63_2-215. In particular, low profile drag is desired over the range from $c_l = 0.1$ at $R = 9 \times 10^6$ (the cruise condition) to $c_l = 0.6$ at $R = 4 \times 10^6$ (the climb condition). While the new airfoil can be used with flaps, it is required that without flaps $c_{l,max} \geq 1.5$ at $R = 2.6 \times 10^6$ (the takeoff/landing condition). In case of surface contamination, the loss in $c_{l,max}$ should be no larger than 14%, the same as that suffered by the NACA 23015. To minimize trim drag penalities, it is desired that $c_{m,o} > -0.055$. Furthermore, for a control surface of 0.2c, the hinge moment coefficient should be no less than that of the NACA 63_2-215, $c_H > -0.0022$. In this case stick forces and control surface "float" will not be excessive. Lastly, the airfoil thickness is set at 15%.

DESIGN PROCEDURE

The airfoil-design process was carried out using the Eppler Airfoil Design and Analysis Program[3]. Briefly, the design method employs inverse conformal mapping to obtain the airfoil through specification of the velocity distribution. It is particularly valuable as a design tool in that it allows different parts of the airfoil to be designed for different operating conditions. In this way, the desired performance envelope is a consequence of the actual design effort rather than that which is obtained when a point-designed airfoil is operated off-design. The analysis method implemented in the program uses the integral boundary-layer momentum and energy equations to predict airfoil performance. Transition is predicted by a method which will be discussed later. The iterative process of designing and analyzing candidate airfoils is

concluded when the airfoil-design objectives and constraints are satisfied and the performance maximized.

NASA NLF(1)-0115 AIRFOIL AND COMPARISONS

The result of the present design effort is the NASA NLF(1)-0115 †, shown in figure 1 along with three inviscid velocity distributions corresponding to the key flight conditions: cruise, climb, and takeoff/landing. The accompanying theoretical airfoil characteristics are shown in figure 2 for $R = 9 \times 10^6$ and 4×10^6, the cruise and climb conditions, respectively. The zero-lift pitching- and hinge-moment coefficients fall within the design specifications, $c_{m,o} = -0.055$ and $c_H = -0.0022$ for a 0.2c control surface. The airfoil thickness is 15% as desired.

A comparison between the airfoil characteristics of the NASA NLF(1)-0115 and those of the NACA 23015 at the cruise flight Reynolds number is presented in figure 3. As seen, the design goal of maintaining a broad lift range like that of the NACA 23015 has been obtained. The low-drag benefit due to laminar flow is achieved in the cruise-flight lift-coefficient range of the new airfoil. It should be noted that one of the prices paid for the lower drag coefficient is an increase in the nose-down pitching-moment coefficient.

The effects of surface contamination are shown in figure 4 for the takeoff/landing Reynolds number of 2.6×10^6. It is observed that the predicted value of $c_{l,max}$ for the NLF(1)-0115 airfoil is not overly sensitive to surface roughness. In fact the lift loss due to contamination is only 11% as compared with 14% for the NACA 23015.

In order to have limited sensitivity to surface roughness, the NLF(1)-0115 airfoil embodies upper-surface velocity distributions which behave as generally depicted in figure 5. The velocity distribution for $c_l = 0.6$ (the upper limit of the low-drag range at $R = 4 \times 10^6$) is prescribed such that with increasing angles of attack the transition point moves rapidly forward to the leading edge from a point just upstream of the main pressure recovery at the midchord. Thus for $c_l < 0.6$, the pressure gradients confine transition to the short instability region just upstream of the main pressure recovery. For $c_l > 0.6$, however, the adverse pressure gradient over the forward portion of the airfoil moves transition to very near the leading edge. Consequently, because turbulent flow is predominate on the upper surface at the maximum lift coefficient, $c_{l,max}$ is not dramatically influenced by surface roughness.

In figure 6, a comparison is made between the airfoil characteristics of the NASA NLF(1)-0115 and those of the NACA 63_2-215 at $R = 9 \times 10^6$ At the cruise condition ($c_l = 0.1$), the NLF(1)-0115 airfoil has 25% less drag than the NACA 63_2-215, and this advantage is maintained over most of the operational envelope. Although both airfoils are designed to have significant runs of laminar flow, significant differences exist in the way in which this is achieved. These differences are best interpreted using the theoretical boundary-layer development plot, such as that shown in figure 7, which requires some preliminary discussion.

In figure 7, the local Reynolds number based on the momentum thickness and local boundary layer edge velocity (R_{δ_2}) is plotted against the shape factor based on the energy and momentum

† Coordinates for the NASA NLF(1)-0115 airfoil may be obtained directly from the authors.

thickness (H_{32}). Note that the logarithmic scale for R_{δ_2} has the tendency to expand the boundary layer near the leading edge and compress it downstream. Starting from the airfoil stagnation point, R_{δ_2} increases monotonically along the upper and lower surfaces of the airfoil. The value of H_{32} can vary significantly, although certain values correspond to specific, laminar boundary-layer phenomena. An H_{32} of 1.620 corresponds to stagnation, 1.573 to the flat-plate Blasius boundary layer, and 1.515 to laminar separation. It is noted that H_{32} has the opposite tendency of the perhaps more familiar H_{12}, which contains the displacement thickness rather than the energy thickness. That is H_{32}, unlike H_{12}, decreases from stagnation toward laminar separation.

The Eppler method of predicting transition is based on the local values of H_{32} and R_{δ_2}. Within the dotted-line boundaries given in figure 7, the flow is assumed to be laminar. The vertical boundary to the left corresponds to laminar separation ($H_{32} = 1.515$), while the upper transition-criterion curve corresponds to natural boundary-layer transition. This transition criterion was emperically derived from wind tunnel and flight test data, and should therefore be considered as a band since it is merely a fairing through the experimental data points. Once transition is predicted, the method switches to the turbulent boundary-layer equations.

The two boundary-layer developments shown in figure 7 are for the upper surface of the NACA 63_2-215 at $c_l = 0.4$ and 0.8 for $R = 4 \times 10^6$. In the figure both boundary-layer developments begin in the lower right at the stagnation point (point A). For $c_l = 0.4$, the curve meets the transition-criterion curve (point B) at which location transition is assumed to take place. As the angle of attack increases, the boundary-layer development curves skew toward the left as the pressure gradients become steeper. For $c_l = 0.8$, the steep adverse pressure gradient immediately downstream of the velocity peak near the leading edge (point C) results in a more rapid decrease in H_{32} and causes transition via a laminar separation bubble.

When the boundary-layer data is provided in this fashion, it reveals valuable information relating to transition and thereby offers clues as to how to sustain laminar flow in the design of a new airfoil. For example, referring back to figure 7 at $c_l = 0.8$, transition is predicted to occur immediately downstream of the stagnation point. If the adverse pressure gradient in the region were reduced through modification of the velocity distribution, transition would be postponed. By adjusting the velocity distribution based on the boundary-layer development plot, laminar flow can be extended further back on the airfoil and is limited only by boundary-layer separation or one of the design constraints. As discussed by Somers[4] and first suggested by Eppler, the widest possible low-drag range is achieved when the laminar boundary layer is held on the verge of laminar separation and then on the verge of boundary-layer transition. Such a scenario would be characterized by a boundary-layer development that follows the dotted lines in figure 7. This concept has been exploited in the design of other airfoils, such as those presented in Refs. 5–7, and is now employed in the NLF(1)-0115.

Figure 8 shows the boundary-layer development for the lower surface of the NLF(1)-0115 at $c_l = 0.0$ and $R = 9 \times 10^6$ and corresponds to the lower limit of the low-drag range (see figure 2). First the laminar-separation limit is approached quickly and is followed for a short distance up to point A. The boundary-layer development then essentially follows the transition-criterion curve. The beginning of the pressure recovery at point B causes the transition criterion to be satisfied which, in turn, invokes the turbulent boundary-layer calculations.

For the upper surface, the critical design condition occurs at the upper limit of the low-drag range. The corresponding boundary-layer development is shown in figure 9 for $c_l = 0.6$ and $R = 4 \times 10^6$. Unlike the design of the lower surface, the upper surface is not designed to rapidily approach laminar separation. Rather from the stagnation point to 0.1c, the design of the upper surface is dictated by $c_{l,max}$ and surface roughness considerations as previously discussed. From 0.1c to 0.5c, however, the boundary layer is again forced to be everywhere on the verge of transition.

Based on this discussion, it should be clear that if the design specifications were altered somewhat, this would warrant a different airfoil. For example, if the upper limit of the low-drag range was desired to occur at $c_l = 0.7$ and $R = 3 \times 10^6$, then this would mainly require modification of the upper-surface velocity distribution while simultaneously keeping within the other constraints. Put simply, for maximum performance, the airfoil should be tailored specifically to its mission requirements.

CONCLUSIONS

The latest in a series of natural laminar-flow airfoils designed at NASA Langley Research Center, the NASA NLF(1)-0115, is intended for use in general-aviation applications where high speed and long range are paramount. Incorporated into this design are favorable features derived from several previously existing successful airfoils. These features, coupled with significant drag reductions made possible through the use of extended lengths of laminar flow, should prove to make the NLF(1)-0115 airfoil successful in application to general-aviation aircraft.

ACKNOWLEDGEMENTS

The support of the NASA Langley Research Center under Grant NGT-50341 is gratefully acknowledged.

REFERENCES

1. Holmes, B.J., Obara, C.J., and Yip, L.P., "Natural Laminar Flow Experiments on Modern Airplane Surfaces," NASA TP-2256, 1984.

2. Abbott, I.H., von Doenhoff, A.E., Theory of Wing Sections, Dover Publications, New York, 1959.

3. Eppler, R. and Somers, D.M., "A Computer Program for the Design and Analysis of Low-Speed Airfoils," NASA TM-80210, 1980.

4. Somers, D.M., "Subsonic Natural-Laminar-Flow Airfoils," in Natural Laminar Flow and Laminar Flow Control, edited by R.W. Barnwell and M.Y. Hussaini, Springer-Verlag, to be published.

5. Somers, D.M., "Design and Experimental Results for a Flapped Natural-Laminar-Flow Airfoil for General Aviation Applications," NASA TP-1865, 1981.

6. Somers, D.M. and Horstmann, K.H., "Design of a Medium-Speed, Natural-Laminar-Flow Airfoil for Commuter Aircraft Applications," Institut fur Entwurfsaerodynamik, Braunschweig, IB 129-85/26, April 1985.

7. Maughmer, M.D. and Somers, D.M. "Design and Experimental Results for a High-Altitude, Long-Endurance Airfoil," J. of Aircraft, Vol. 26, No. 2, Feb. 1989, pp. 148–153.

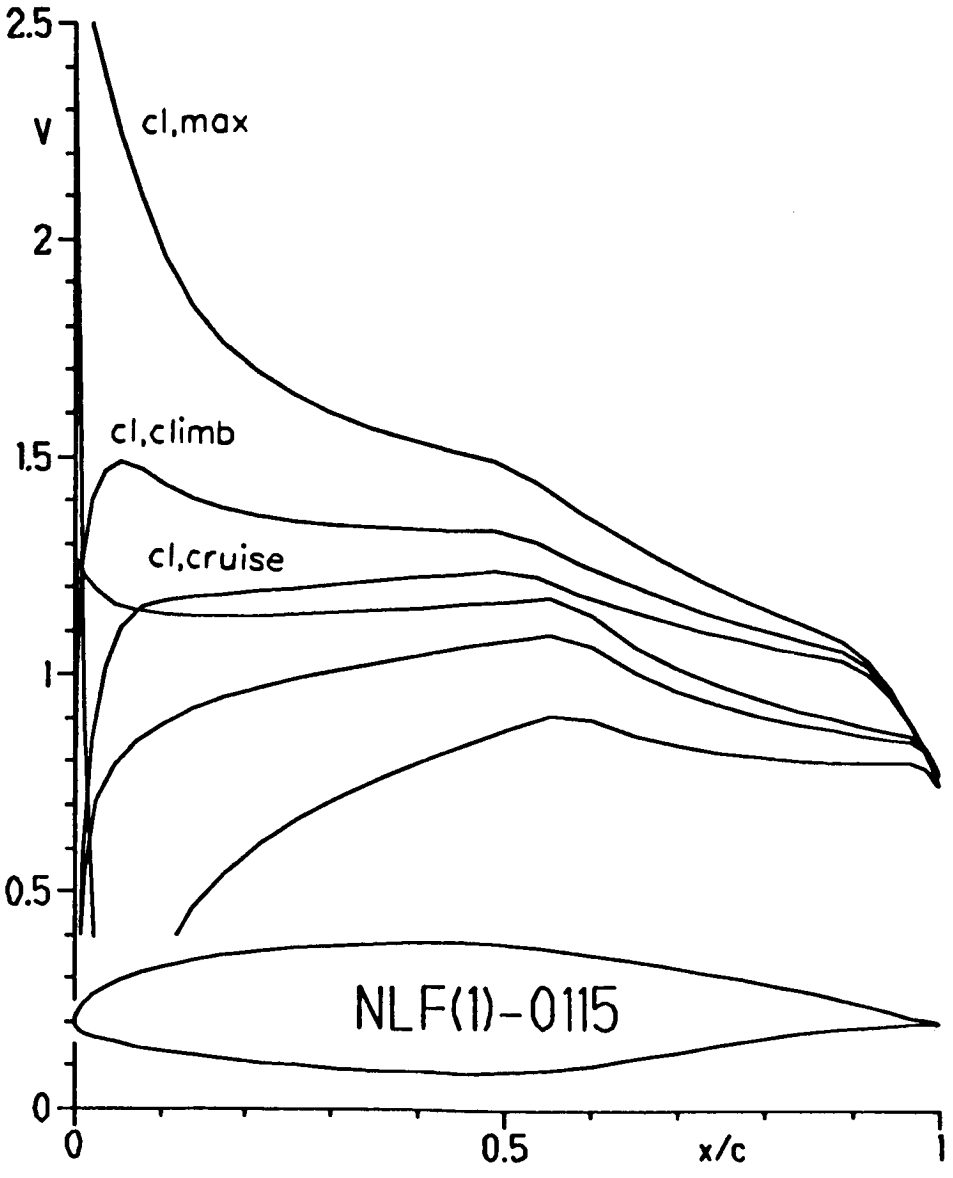

Figure 1. NASA NLF(1)-0115 airfoil and three inviscid velocity distributions.

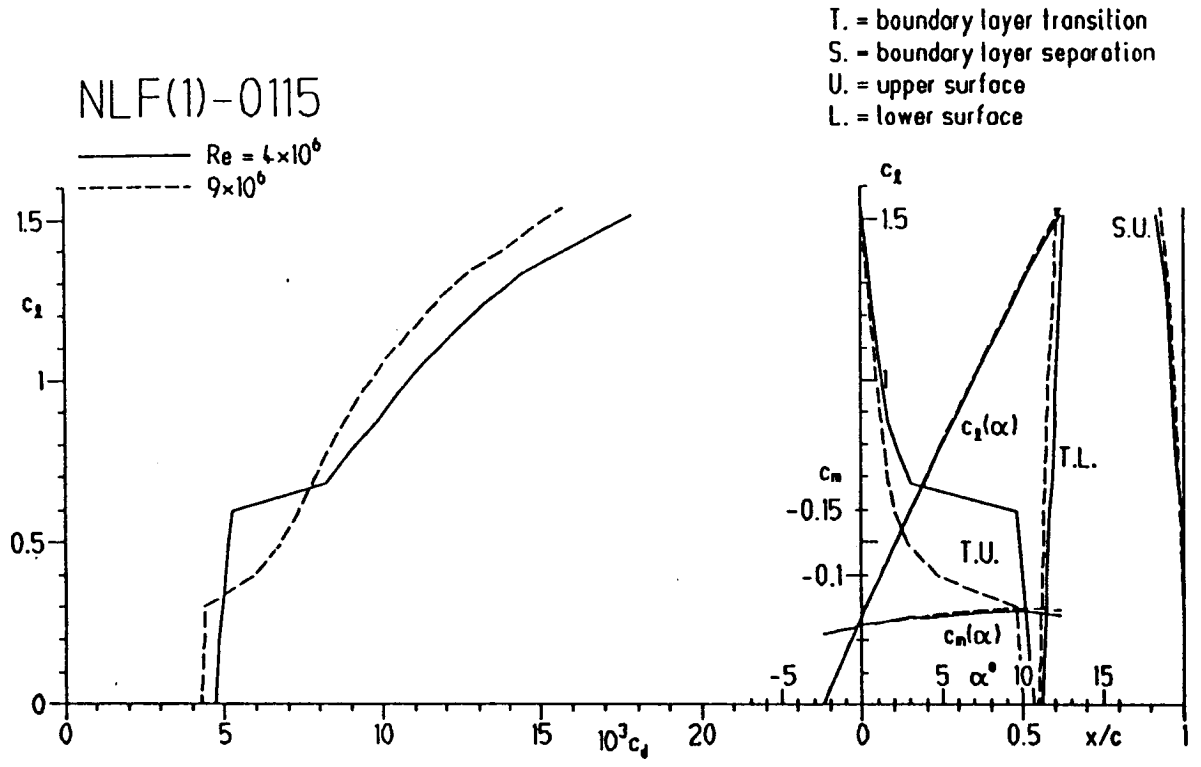

Figure 2. Theoretical airfoil characteristics for the NASA NLF(1)-0115 airfoil.

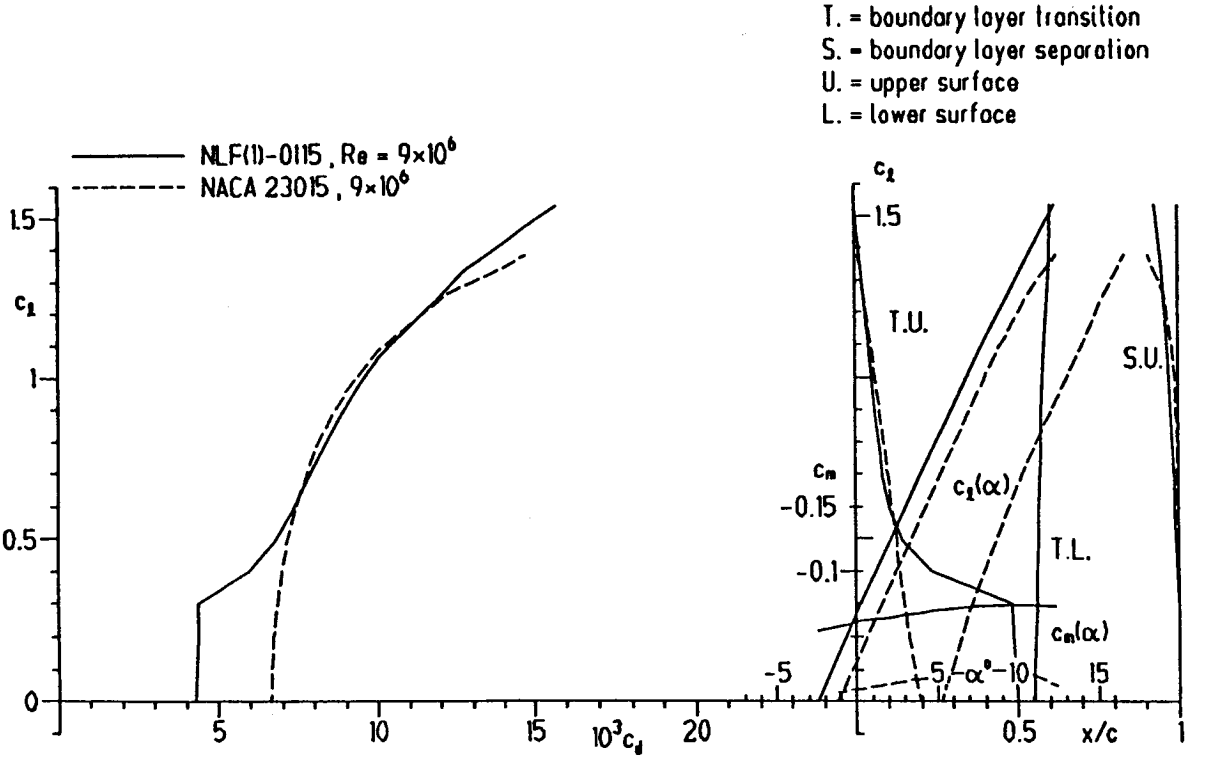

Figure 3. Comparison of the NASA NLF(1)-0115 and NACA 23015 theoretical airfoil characteristics for $R = 9 \times 10^6$.

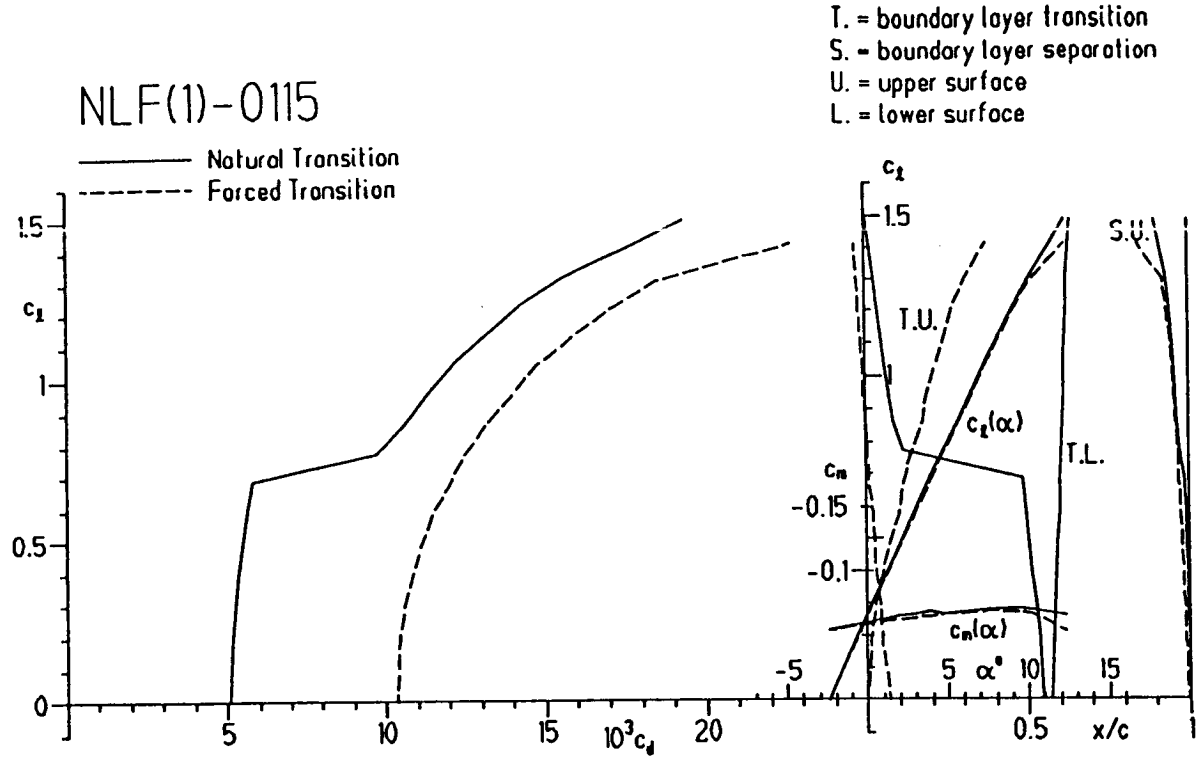

Figure 4. The effects of surface roughness on the theoretical airfoil characteristics of the NASA NLF(1)-0115 airfoil for $R = 2.6 \times 10^6$.

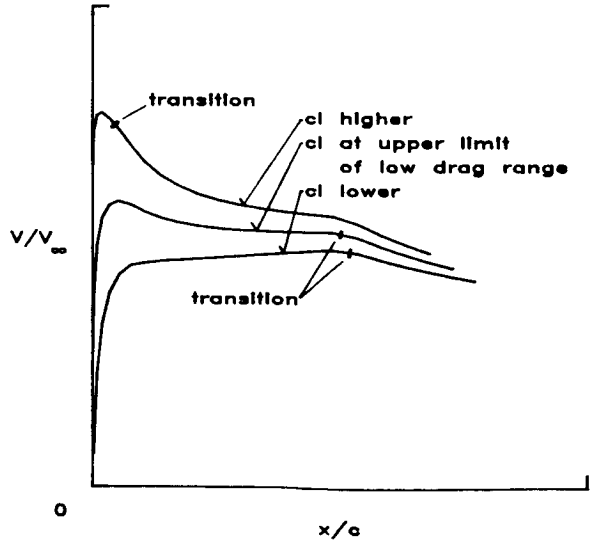

Figure 5. Behavior of the upper-surface velocity distribution that limits $c_{l,max}$ sensitivity to surface roughness.

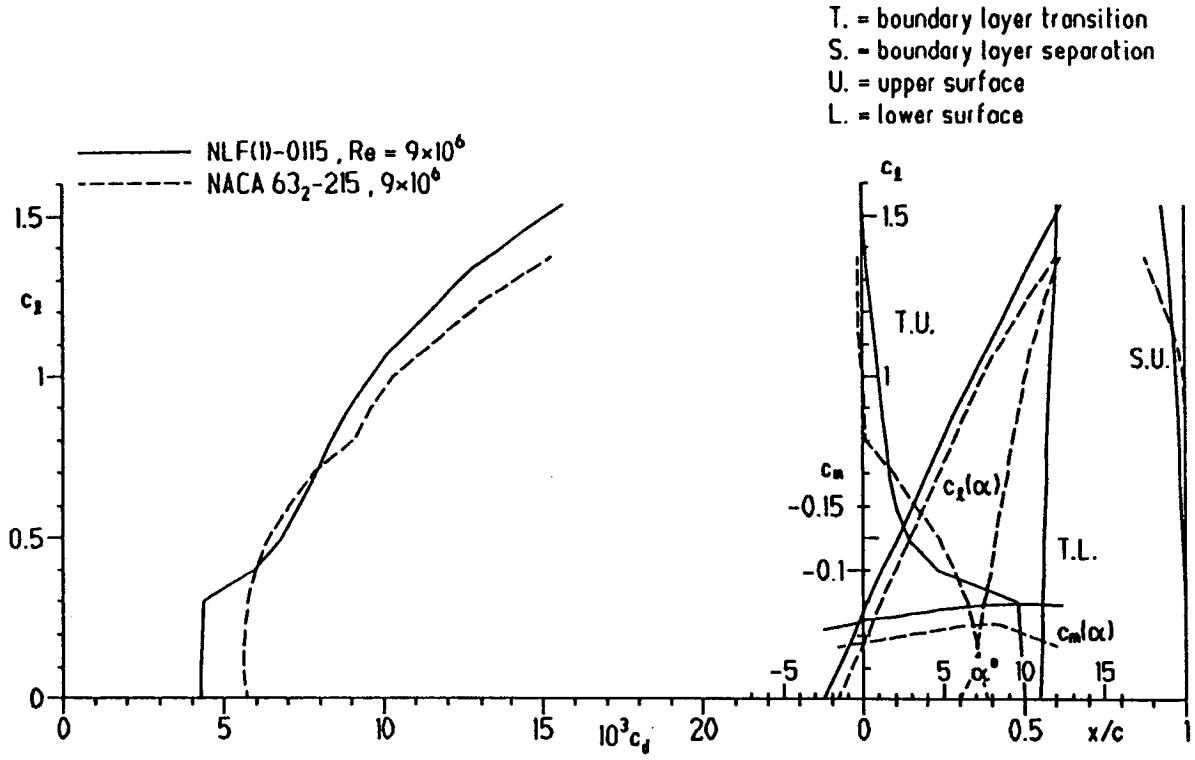

Figure 6. Comparison of the NASA NLF(1)-0115 and NACA 63_2-215 theoretical airfoil characteristics for $R = 9 \times 10^6$.

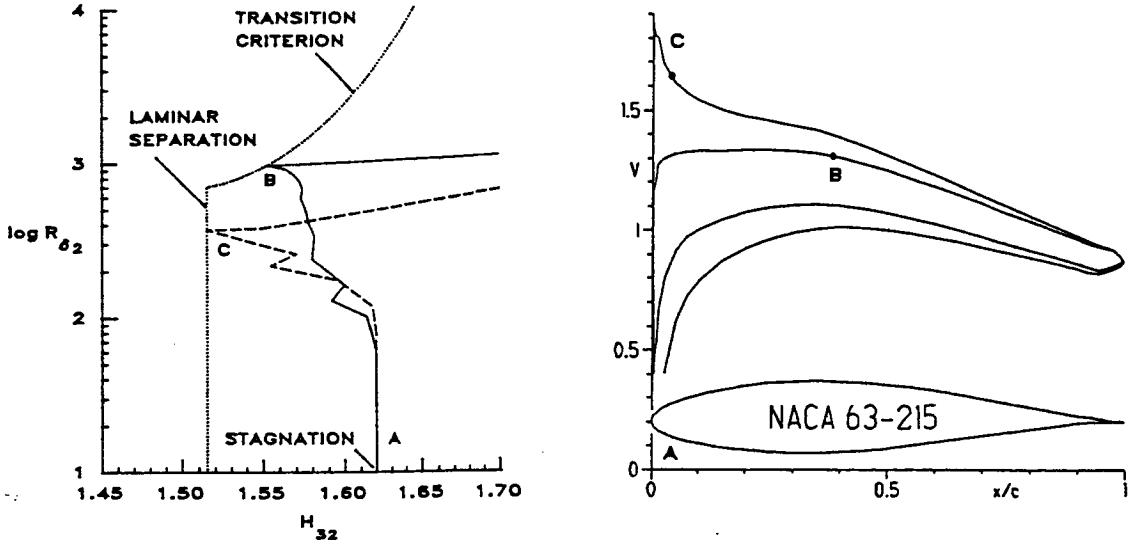

Figure 7. Theoretical boundary-layer development for the NACA 63_2-215 airfoil lower surface at $c_l = 0.4$ (solid-line) and 0.8 (dotted-line) for $R = 4 \times 10^6$.

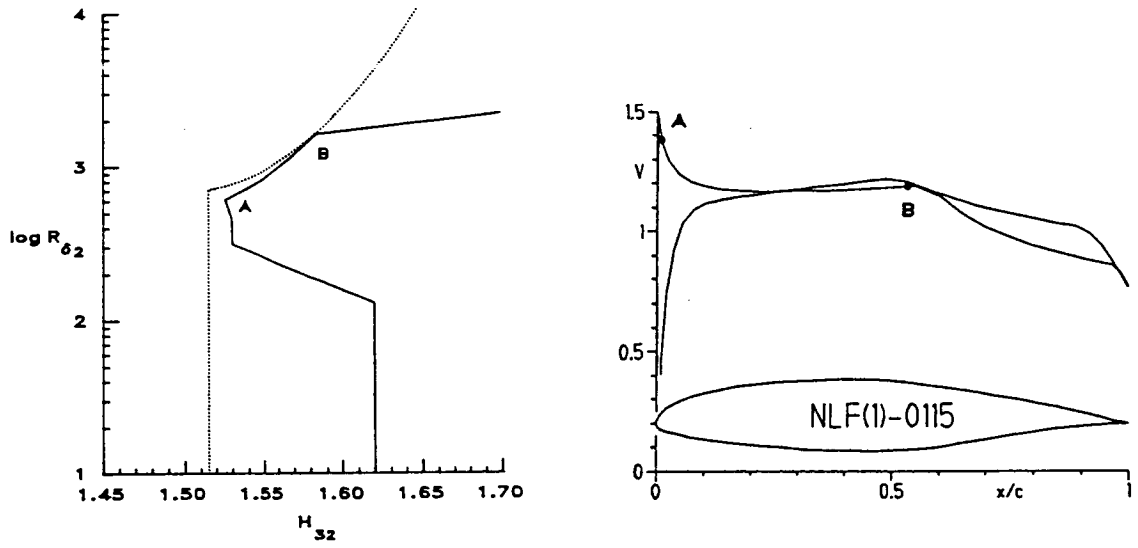

Figure 8. Theoretical boundary-layer development for the NASA NLF(1)-0115 airfoil lower surface at $c_l = 0$ and $R = 9 \times 10^6$.

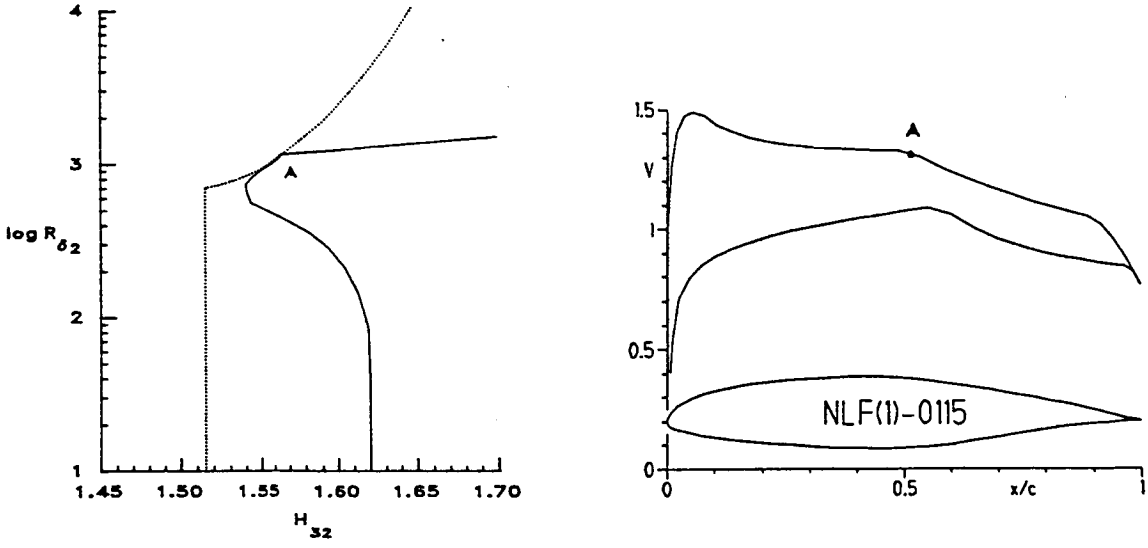

Figure 9. Theoretical boundary-layer development for the NASA NLF(1)-0115 airfoil upper surface at $c_l = 0.4$ and $R = 4 \times 10^6$.